# Supplementary Material

**Amyloidogenic Nanoplaques in Cerebrospinal Fluid: Relationship to Amyloid Brain Uptake and Clinical Alzheimer's Disease in a Memory Clinic Cohort**

## Instrumental Setup and Calibration

Fluorescence correlation spectroscopy (FCS) measurements were performed using an individually modified ConfoCor 3 system (Carl Zeiss, Jena, Germany), consisting of an inverted microscope for transmitted light and epifluorescence (Axiovert200M); theVIS-laser module comprising the Ar-ion (458, 477, 488, and 514 nm), the HeNe 543 nm and the HeNe 633 nm lasers; scanning module LSM 510 META modified to enable detection in the imaging mode using silicone avalanche photodiodes (SPCM-AQR-1X;PerkinElmer) and the FCS module with 3 detection channels [1]. Fluorescence intensity fluctuations were examined by temporal autocorrelation analysis, using the program for online FCS data analysis that is part of the ConfoCor3 running software package. The thus generated temporal autocorrelation curves (tACCs) were evaluated using the same software package, but also offline using the Maximum Entropy Method based fitting routine for FCS (MEMFCS) that is specifically developed for bias-free fitting of FCS measurements in highly heterogeneous biological systems [2, 3].

Thioflavin T (ThT) fluorescence was excited using the 458 nm line of the Ar-ion laser. The HFT 458/514 main dichroic beam splitter was used to separate the incident and the emitted light. The BP 530-610 emission filter was used in front of the avalanche photodiode detector, and the pinhole size was 70 µm (1 Airy). Standard solutions of Rhodamine 6G (Rh6G), 5–25 nM, were used for instrument calibration. For this purpose, the same optical setting as for ThT was used for Rh6G. The tACC for Rh6G standard solution (Supplementary Figure 1A) was fitted using the MEMFCS fitting routine for FCS (Supplementary Figure B). The diffusion time of Rh6G was determined to be $\tau_{D,Rh6G}$ = (29 ± 2) µs ($n$ = 30 independent

calibration measurements, each measurement containing 10 consecutive 10 s repeats), the count per molecule and second (CPMS) was CPMS = (10.2 ± 0.7) kHz, and the structure parameter was 6 ± 1.

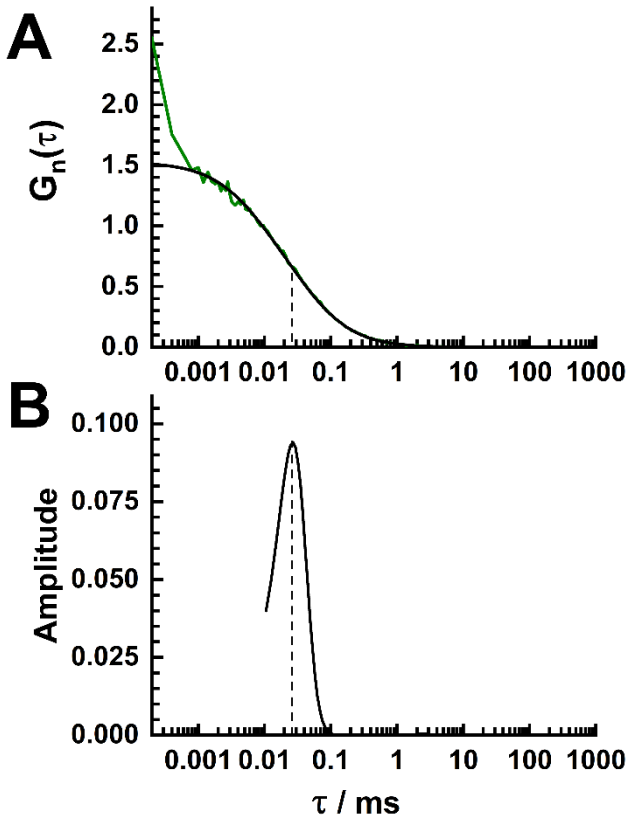


**Supplementary Figure 1.** A) Experimentally derived temporal autocorrelation curve for Rhodamine 6G (Rh 6G) normalized to $G_n(\tau) = 1$ at lag time $\tau = 10$ µs, (green) obtained using the optical setting for Thioflavin T (ThT). The corresponding best-fit curve derived by MEMFCS (black). B) Diffusion time of Rh6G, determined by MEMFCS is $\tau_{D,Rh6G} = (29 \pm 2)$ µs.

**Determining the Concentration and Size of Nanoplaques by Fluorescence Intensity Fluctuation Analysis**

ThT fluorescence intensity fluctuations were collected with a temporal resolution of 50 ns. To minimize photobleaching, the signal was collected in 30 series of 10 consecutive measurements, each uninterrupted measurement lasting 10 s, with a 5 min break between the series. In this way, the total signal acquisition time was always 3000 s.

Time-resolved detection of ThT fluorescence in the CSF (Supplementary Figure 2) revealed fluorescence intensity fluctuations with short (Supplementary Figure 2A) and long (Supplementary Figure 2B) characteristic times, which are easily discernible by temporal autocorrelation analysis (Supplementary Figure 2C) and MEMFCS (Supplementary Figure 2D).

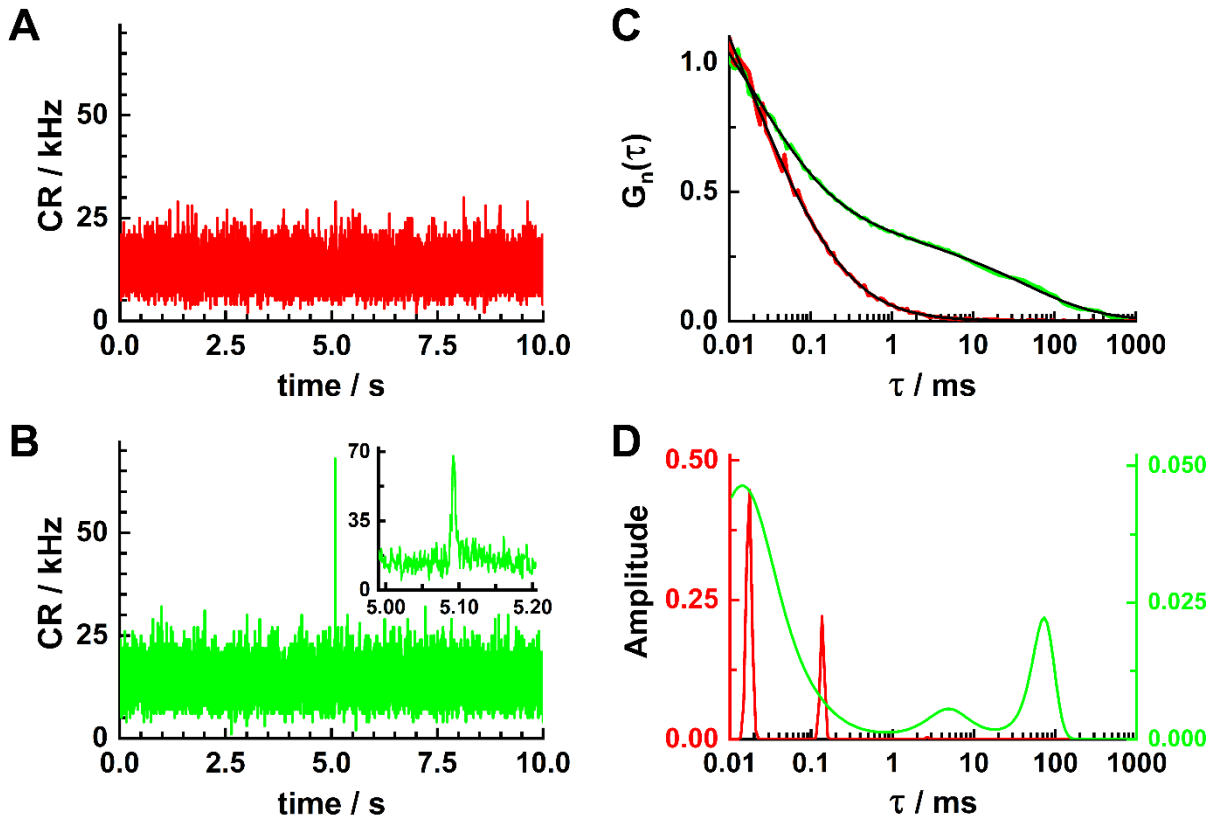


**Supplementary Figure 2.** A) Time-resolved fluctuations in ThT fluorescence generated by free diffusion of small autofluorescent/weakly ThT-responsive molecules in the CSF. B) Time-resolved fluctuations in ThT fluorescence showing amid small-amplitude fluorescence intensity fluctuations a large fluorescence intensity peak (magnified in the inset) that reflects the occasional passage of a bright ThT-labeled structured amyloidogenic aggregate, i.e., a nanoplaque, through the observation volume element (OVE). C) Temporal autocorrelation curves (tACCs) normalized to the same amplitude, $G_n(\tau) = 1$ at lag time $\tau = 10$ µs, generated by temporal autocorrelation analysis of time series shown in A (red) and B (green) and corresponding best fits (black) derived using the Maximum Entropy Method based fitting routine for FCS (MEMFCS). D) MEMFCS reveals fast fluorescence intensity fluctuations with a short diffusion time, $\tau_D < 200$ µs, originating from free 3D diffusion of small autofluorescent/weakly ThT-responsive molecules in the CSF that quickly diffuse through the OVE (red), and fluorescence intensity bursts with long diffusion times, 1 ms $< \tau_D <$ 100 ms, reflecting the occasional passage of bright ThT-labeled structured amyloidogenic aggregates, i.e., nanoplaques, that is observed amidst the small molecules' diffusion (green).

Fluorescence intensity fluctuations with a short diffusion time, $\tau_D < 200$ μs (Supplementary Figure 2A), originate from small autofluorescent/weakly ThT-responsive molecules in the CSF that quickly diffuse through the observation volume element (OVE). The rarely observed large fluorescence intensity bursts with long diffusion times, $1 \text{ ms} < \tau_D < 100 \text{ ms}$, that are observed amidst the fast fluorescence intensity fluctuations, reflect the occasional passage of bright ThT-labeled structured amyloidogenic aggregates, i.e., nanoplaques (Supplementary Figure 2B).

To determine the concentration and size of nanoplaques, it is not possible to use the standard temporal autocorrelation analysis procedure—since the concentration of nanoplaques is several orders of magnitude lower than the concentration of small autofluorescent/weakly ThT-responsive molecules, the difference in their relative amplitudes is rather large and the information about the nanoplaques' concentration and diffusion are "hidden" in the small-amplitude tail of the tACC. To circumvent this problem, an automated procedure is first used to determine whether in an uninterruptedly collected 10 s time series an increase in fluorescence intensity by a value that is more than five times larger than the standard deviation of the whole time series, is observed. These peaks in fluorescence intensity, termed "single events", reflect the passage of a single nanoplaque. To determine the frequency of single event occurrence, *f*seo, the number of "single events" observed in each 10 s measurement is counted, these values are summed and the *f*seo is calculated by normalizing the total number of "single events" to the total measurement time length (3000 s). The *f*seo is a direct measure of the concentration of nanoplaques in the CSF, as shown in [4]. Using the calibration curve shown in Supplementary Figure 3 in [4], the average concentration of nanoplaques in the CSF, *f*seo = 17.4 (11.4-24; Table 1) is estimated to be in the fM range, about $7.5 \times 10^{-15}$ M (5 – 10.5 fM).

To analyze the size of amyloid-β (Aβ) aggregates, tACCs were generated for time series where "single events" were observed. The tACCs were then normalized to the same amplitude, $G_n(\tau) = 1$ at lag time $\tau = 10$ µs, and averaged. Given that a small number of "single events" was observed for each individual, average tACCs for each patient group: amyloid-negative, amyloid-positive, AD and non-AD, were derived (Supplementary Figure 3A). The thus generated tACCs were evaluated using MEMFCS, to determine the distribution of diffusion times, which also reflects the distribution of sizes (Supplementary Figure 3B).

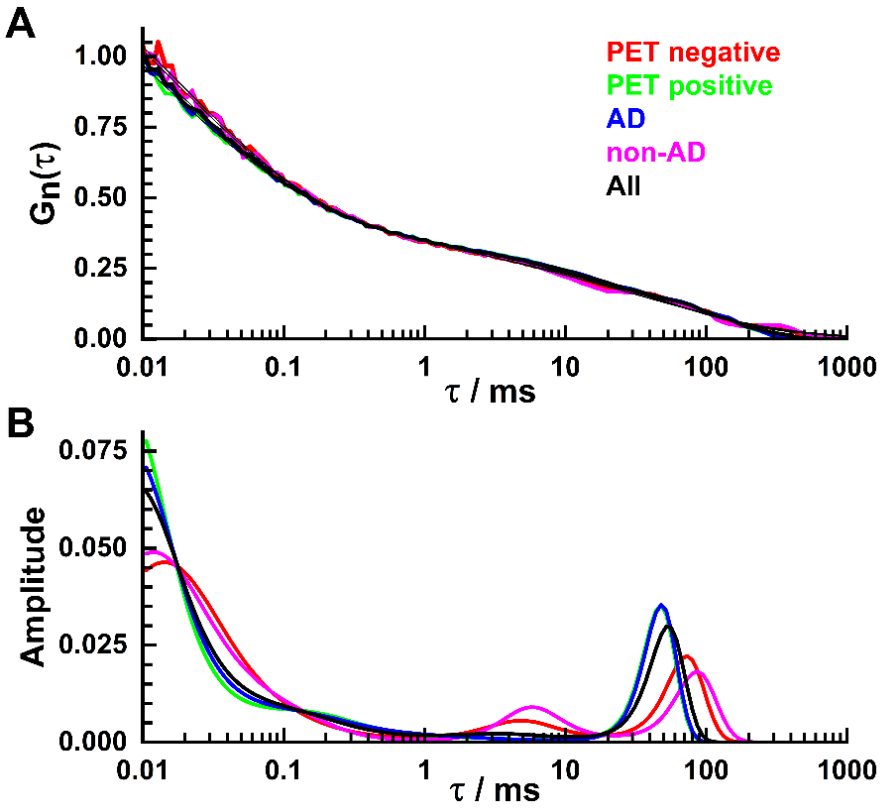


**Supplementary Figure 3.** A) Temporal autocorrelation curves (tACCs) where single-event occurrence was observed normalized to the same amplitude, $G_n(\tau) = 1$ at lag time $\tau = 10$ µs, and averaged across different groups: amyloid negative (red), amyloid positive (green), AD (blue) and non-AD (magenta). B) MEMFCS reveals presence of medium-sized, 1 ms < $\tau_D$ < 4 ms, and large, 30 ms < $\tau_D$ < 100 ms, ThT-responsive aggregates in all patient groups.

From the experimentally measured diffusion times of nanoplaques, 1 ms < $\tau_{D,nanoplaques}$ < 100 ms (Supplementary Figure 3B), and the calibration experiments with Rh6G (Supplementary Figure 1), the diffusion coefficients of nanoplaques, $D_{nanoplaques}$, could be determined: $D_{nanoplaques} = \tau_{D,Rh6G} \cdot D_{Rh6G}/\tau_{D,nanoplaques}$, where $\tau_{D,Rh6G} = (29 \pm 2)$ µs and the diffusion coefficient of Rh6G is $D_{Rh6G} = 4.14\times10^{-10}$ $m^{-2}s^{-1}$, yielding $1.2\times10^{-13}$ $m^2s^{-1} < D_{nanoplaques} < 1.2\times10^{-11}$ $m^2s^{-1}$. Assuming the rigid sphere approximation, the Stokes-Einstein relation $D = kT/6\pi\eta r$, where: k is the Boltzmann constant, $k = 1.38\times10^{-23}$ J/K, T is the absolute temperature, T = 293 K, η is the viscosity of water, $\eta = 1.002\times 10^{-3}$ kg/m·s, and r is the hydrodynamic radius of the molecule, can be applied to derive the theoretical relationship between the molecular mass (m) and the diffusion coefficient: $D \propto \sqrt[3]{\frac{1}{m}}$ (for full derivation see reference [5]). By using a standard molecule, in this case Rh6G, as a reference, the following relationship can be derived $(D_{Rh6G}/D_{nanoplaques})^3 = m_{nanoplaques}/m_{Rh6G}$. Thus, by knowing the molecular mass and diffusion coefficient of a molecule used for system calibration, in this case Rh6G, an average molecular mass of nanoplaques could be estimated using this relationship, yielding: $2\times10^4$ kDa < $m_{nanoplaques} < 2\times10^{10}$ kDa. For elongated, rod-like molecules with a length (L) and diameter (d), the length-to-diameter (L/d) aspect ratio needs to be accounted for. Applying the correction: $A = \ln(L/d) + 0.312 + 0.565/(L/d) - 0.1/(L/d)^2$ [5], the correction factor A can be calculated for different length-to-diameter aspect ratios to assess more precisely the average molecular mass of the nanoplaques. Given that statistically significant differences were not observed in the nanoplaques' size between different patient groups, nanoplaque size was not further analyzed.

**CSF Storage Time Does Not Affect the Results of ThT-FCS Analysis**

The sample storage time, ranging from about three months to about three years, did not significantly affect the results of ThT-FCS analysis (Supplementary Figure 4).

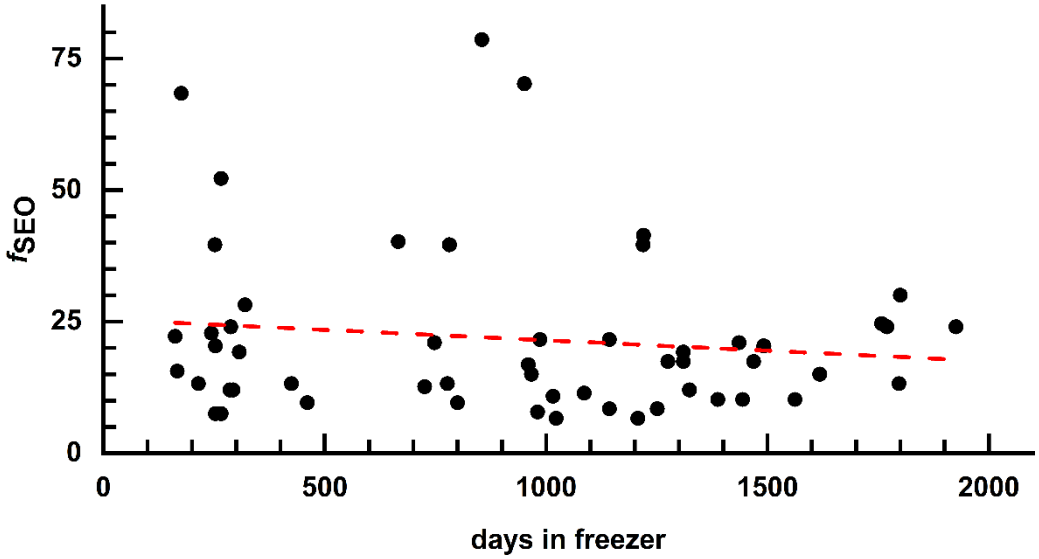


**Supplementary Figure 4.** Scatter plot showing the relationship between nanoplaque levels (*f*SEO) in the CSF as a function of CSF sample storage time at – 80°C. The association between the two variables was not statistically significant, as evident from the Spearman's rank correlation coefficient, ρ = -0.07023, and the 2-tailed *p*-value, *p* = 0.61381 (calculated using the online Spearman's Rho Calculator (https://www.socscistatistics.com/tests/spearman/default2.aspx).

**Supplementary Table 1.** Summary of linear regression models with the ratio of standardized uptake values from a target and a reference region (SUVR) as the dependent variable.

| Characteristic | Univariate model | | Clinical model | | Full model | |
|---|---|---|---|---|---|---|
| | B (95% CI) | *p* | B (95% CI) | *p* | B (95% CI) | *p* |
| Log *fSEO* | 0.05 (-0.20-0.29) | 0.70 | - | - | 0.02 (-0.18-0.23) | 0.84 |
| Age | - | | 0.01 (0.01-0.03) | 0.31 | 0.01 (-0.01-0.03) | 0.31 |
| Male sex | - | | -0.60 (-0.85- -0.34) | <0.001 | -0.59 (-0.85- -0.33) | <0.001 |
| MMSE | - | | -0.01 (-0.04-0.02) | 0.37 | -0.01 (-0.05-0.02) | 0.36 |
| APOE e4 | - | | 0.11 (-0.17-0.38) | 0.45 | 0.11 (-0.18-0.39) | 0.45 |
| $R^2$ | | 0.003 | | 0.39 | | 0.39 |
| Adjusted $R^2$ | | -0.018 | | 0.32 | | 0.32 |

Linear regression models were used to assess predictors of SUVR after adjustment by selected covariates in 50 patients.

The univariate model included only log *fSEO* as a predictor; the clinical model included age, sex, MMSE, and *APOE* ε4 status; the full model combined the univariate and clinical model.

*APOE*, apolipoprotein; B, beta-coefficient; CI, confidence intervals; *f*SEO, frequency of single event occurrence; MMSE, Mini-Mental State Examination.

## REFERENCES


[1] Vukojević V, Heidkamp M, Ming Y, Johansson B, Terenius L, Rigler R (2008) Quantitative single-molecule imaging by confocal laser scanning microscopy. *Proc Natl Acad Sci U S A* **105,** 18176-18181.

[2] Sengupta P, Garai K, Balaji J, Periasamy N, Maiti S (2003) Measuring size distribution in highly heterogeneous systems with fluorescence correlation spectroscopy. *Biophys J* **84**, 1977-1984.

[3] Krieger JW, Langowski J. QuickFit 3.0 (status: beta, compiled Oct 29, 2015, SVN: 4465): A data evaluation application for biophysics, https://www.dkfz.de/Macromol/quickfit/, Accessed January 2020.

[4] Tiiman A, Jelić V, Jarvet J, Jaremo P, Bogdanović N, Rigler R, Terenius L, Graslund A, Vukojević V (2019) Amyloidogenic nanoplaques in blood serum of patients with Alzheimer's disease revealed by time-resolved Thioflavin T fluorescence intensity fluctuation analysis. *J Alzheimers Dis* **68**, 571–582.

[5] Krouglova T, Vercammen J, Engelborghs Y (2004) Correct diffusion coefficients of proteins in fluorescence correlation spectroscopy. Application to tubulin oligomers induced by $Mg^{2+}$ and paclitaxel. *Biophys J* **87**, 2635–2646.